Clim Dyn (2008) 31:417–432
DOI 10.1007/s00382-007-0327-9

Seasonal rotation features of wind vectors and application to evaluate monsoon simulations in AMIP models

Li Zhang · Jianping Li

Received: 5 October 2006 / Accepted: 16 September 2007 / Published online: 30 October 2007

Abstract A new concept, the directed angle, is introduced to study seasonal rotation regimes of global wind vectors and annual variability of monsoon. Compared with previous studies on using angles between wind vectors, this concept better describes the daily variations of both rotation direction and rotation amplitude of wind vector. According to the concept, six categories of wind vector rotation with seasonal cycle in the global have been detected and classified as follows: (1) Clockwise to counter-clockwise (CTCC) rotation; (2) Counter-clockwise to clockwise (CCTC) rotation; (3) Full clockwise (FC) rotation; (4) Full counter-clockwise (FCC) rotation; (5) Stable style; (6) Unstable style. Generally, wind vectors in monsoon regions rotate in forms of the first four styles. Moreover, the rotation direction and rotation amplitude of wind vectors have regional differences, and different monsoon subsystems possess different rotation styles for wind vectors in an annual cycle. For instance, the South Asian monsoon follows the CCTC rotation, while the East Asian monsoon follows the FCC rotation. The CTCC rotation is seen in the South China Sea. Both the West Africa and the South Indo-China Peninsula are covered by the FC rotation. Therefore, the directed angle is able to describe the evolution of wind vectors on a daily scale, which provides a new clue for spatio-temporal information about wind vector variation and model evaluation. Using the new concept, this study aims at evaluating the model outputs of eight AGCMs of AMIP in the Intergovernmental Panel on Climate Change (IPCC) Fourth Assessment Report (AR4). Compared to the corresponding observations, most models are able to simulate the global rotation regimes of wind vectors reasonably well, however very little skill is shown in the monsoon rotation styles of some models, especially in the South China Sea and West Africa. Moreover, the simulations differ mostly from observations during the transitional season.

This paper is a contribution to the AMIP-CMIP Diagnostic Subproject on General Circulation Model Simulation of the East Asian Climate, coordinated by W.-C. Wang.

L. Zhang · J. Li
State Key Laboratory of Numerical Modeling for Atmospheric Sciences and Geophysical Fluid Dynamics (LASG), Institute of Atmosphere Physics, Chinese Academy of Sciences, Beijing 100029, China

L. Zhang
Graduate University of Chinese Academy of Sciences, Beijing 100049, China

J. Li (✉)
LASG, Institute of Atmospheric Physics, Chinese Academy of Sciences, P.O. Box 9804, Beijing 100029, China
e-mail: ljp@lasg.iap.ac.cn

1 Introduction

As an ancient climatological concept, the monsoon is characterized by the seasonal reversal of prevailing surface winds, and the alternation between a rainy summer and a dry winter (Ramage 1971; also see reviews about monsoons in the Encyclopedia of Atmospheric Sciences, Holton 2003). Monsoon defines essential features of the Earth's climate which have profound social and economic consequences. Studies on the annual cycle of monsoons, their onset time, as well as the variabilities of their intensity are of great scientific and societal importance. Furthermore, their importance to global circulation and climate

predictability is widely recognized, and a series of projects have been set up and developed to accelerate further studies of monsoons; for example, the Summer Monsoon Experiment (MONEX), the Tropical Ocean Global Atmosphere Program (TOGA), the Monsoon Numerical Experimentation Group (MONEG), the Atmospheric Model Intercomparison Project (AMIP), and the Climate Variability and Predictability Study (CLIVAR).

Recently, many general circulation models (GCMs) have been developed and employed to investigate various aspects of monsoons and their prediction (Shukla and Fennessy 1994; Fennessy et al. 1994; Zhang et al. 1997; Webster et al. 1998; Sperber et al. 2000; Lau and Nath 2000; Kang 2004; Wang et al. 2004a, b). Since it is recognized that the Asian summer monsoon, as a key element of global circulation, has important influence on the atmospheric variability of surrounding areas (Zeng et al. 1988; Shukla et al. 1992; Latif et al. 1994; Wang et al. 2004a, b), it is used as a main focus in the present study. A question arises naturally as follows: how well do current climate models perform in simulating the monsoon? Several studies have suggested that simulations of mean monsoon climate and its variations over different timescales are needed for further improvement (e.g. Fennessy et al. 1994; Goswami 1998; Webster et al. 1998; Zachary and Randall 1999; Kang et al. 2002a, b; Waliser et al. 2003). In addition, the results from the AMIP also showed that there are major shortcomings in the ability to simulate even basic aspects of the monsoon by atmospheric general circulation models (AGCMs) [Sperber and Palmer 1996; plus see reviews by Bin Wang (2006)]. Therefore, one of the major future challenges is to understand why climate models show so little ability and how to identify the key physical processes of the monsoon. It indicates that, in order to improve model performance, it is crucial to improve our understanding of the mechanisms involved in the evolution of the monsoon and its spatial and temporal variability through diagnostic observational studies (Annamalai et al. 1999). Furthermore, how to validate the reliability and evaluate the performance of monsoon simulation are also important tasks for model development. So far, most of these techniques concentrate on directly comparing the averaged spatial fields in a certain period (a season or a month), or the averaged temporal fields in a certain area (zonal or meridional), with corresponding observations. Although traditional objective techniques based on point error statistics and correlation coefficients are often used commonly to quantitatively verify the simulated performance (Liu et al. 1994; Rajendran et al. 2004; Wang et al. 2004a, b), these techniques are only useful for validating the simulated mean states of certain variables related to the monsoon; it is difficult for them to reflect the model's performance on reproducing the primary features of spatio-temporal evolution of the monsoon. Furthermore, evaluated climate spatial scales have changed from the global to the regional level in the 1990s, and evaluated temporal scales have changed from long-term-averaged (e.g. monthly, seasonal, or annual) to the variability on a diurnal or daily scale (Zhao et al. 1995).

At present, wind and precipitation are the major variables used for evaluating the simulated performance of a monsoon. In particular, most studies focus on the evaluation of simulated precipitation (Gadgil and Sajani 1998; Kang et al. 2002b), since the major seasonal rain belt and its unusual behavior affected by the summer monsoon can cause extensive drought or flood disasters (Ding 1992). However, it is well known that wind is a vital element influencing variations in pressure, temperature and humidity. Furthermore, although many meteorologists define monsoons according to their own views, seasonal reversal of the wind vector is generally regarded as the common and essential characteristic of monsoons among these viewpoints (e.g. Pedelaborde 1963; Ramage 1971; Khromov 1978; Webster 1987; Krishnamurti 1996). This implies that not only is wind a key element for describing and representing monsoons, but also that variability in wind direction is an essential feature for monsoon characterization. Therefore, understanding the evolution of wind vectors plays an important role in investigating the seasonal variation of monsoons. While great effort should still be devoted to comparing observed and simulated global wind directions, stricter standards and systemic criterions should be employed to validate models, including the spatio-temporal evolution of monsoon wind vectors. In addition, variations in wind direction should also provide a phenomenological-based verification methodology for evaluating the performance of monsoon simulations. Fortunately, the newest AMIP model outputs of the Intergovernmental Panel on Climate Change (IPCC) Fourth Assessment Report (AR4) provide a good opportunity to study the development and improvement of AGCMs. For this purpose, the present study introduces a new concept of directed angle to describe wind direction variability with seasonal evolution, employing it to study annual monsoon variability in order to evaluate the performance of AGCMs in monsoon simulations.

The remaining part of this paper is organized as follows. Section 2 describes the model data obtained from the IPCC AR4 and the observational data used in the present study. In addition, the concept and calculation of directed angle are introduced. Section 3 examines the variability of the global wind vector (especially over monsoon domains) and classifies the rotation regimes based on the directed angle. The rotation regimes and annual evolution of wind

direction over monsoon regions are discussed in Sect. 4. Section 5 assesses the models' ability to reproduce the rotation styles of global wind vector, and focus on the simulated variation of monsoon wind vector. Summary and discussion are given in Sect. 6.

2 Data and methodology

2.1 Data

AMIP is a standard experimental protocol for global AGCMs (see http://www-pcmdi.llnl.gov/projects/amip/index.php). It provides a community-based infrastructure in support of climate model diagnosis, validation, intercomparison, documentation and data access. This framework enables a diverse community of scientists to analyze AGCMs in a systematic fashion, a process which serves to facilitate model improvement. The entire international climate modeling community has participated in this project since its inception in 1990. Daily wind data of model output from AMIP simulation used for the IPCC AR4 have been acquired from different modeling groups and stored at the Program for Climate Model Diagnosis and Intercomparison (PCMDI). Eight institutes from seven countries participated in the intercomparison project, which provided the data for the present study. The descriptions of the participating models are given in Table 1 (see http://www-pcmdi.llnl.gov/ipcc/about_ipcc.php for more information about the models). Because of the different simulation periods in each model, 850 hPa daily wind data from 1 January 1979 to 31 December 1999 are averaged to construct the climatological annual cycle.

In the present analysis, for model validation, we use the National Center for Environmental Prediction/National Center for Atmospheric Research (NCEP/NCAR) reanalysis products (Kalnay et al. 1996). The 850 hPa climatological daily mean wind dataset was constructed for the 21-year period for 1979–1999 with global coverage on 2.5° × 2.5° grids. A 5 day running mean is applied to suppress high frequency variations. Five-point average is employed to eliminate the small-scale features of the rotation regimes.

2.2 Directed angle and its difference with absolute angle

In traditional studies, the angle between two prevailing surface wind vectors is calculated as follows:

$$\beta_j = \beta(\mathbf{V}_j, \mathbf{V}_R) = \arccos\left(\frac{(\mathbf{V}_j, \mathbf{V}_R)}{|\mathbf{V}_j||\mathbf{V}_R|}\right), \quad (j = 1, ..., 365). \tag{1}$$

where $\mathbf{V}_j$ is the daily wind vector, and $\mathbf{V}_R$ is the reference wind vector at the same position. In this study, we choose the January climatological wind vector (one could, however, choose any month) as the reference wind vector. The norm ($\mathbf{V}_j$, $\mathbf{V}_R$) means vector product, and $|\cdot|$ denotes the module of the wind vector. Thus $\boldsymbol{\beta}_j$ essentially measures the contrast of the wind vector angles between a specific day and the corresponding winter. Obviously, $0 \le \beta_j \le 180°$, that is, $\boldsymbol{\beta}_j$ is always positive, so here it is named the absolute angle.

The absolute angle between prevailing surface wind vectors of summer and winter was used to describe and study monsoons in previous studies (e.g. Khromov 1978; Li and Zeng 2000). However, the definition of absolute angle does not include the rotation direction of the wind vector. Actually, the variations in wind direction during seasonal evolution are not consistent in different areas. Figure 1a indicates the scattered representation of normalized wind vectors at (10°N, 55°E). The dots denote the directions of daily wind vectors. It is obvious that the wind vector rotates clockwise from its winter state (Jan 1–May 9) to its summer state (May 16–Oct 8). Then, it continuously rotates clockwise and returns to its initial state. During the whole process, the wind vector rotates clockwise by almost 360°. However, the rotation direction of the wind vector at (15°N, 45°E; see Fig. 1b) is quite different.

Table 1 Information about AGCMs of AMIP in the IPCC AR4

Model	Institution	Resolution	Simulated periods	Experiments
BCC-CM1	Beijing Climate Center, China	T63L16	1979–2003	4
CNRM-CM3	Centre National de Recherches Meteorologiques, France	T42L45	1979–2000	1
GISS-MODEL_E_R	NASA Goddard Institute for Space Studies, America	4° × 5°L20	1979–2000	1
IAP-FGOALS-1.0g	LASG, Institute of Atmospheric Physics, China	2.8125° × 2.8°L26	1979–1999	3
INM-CM3.0	Institute for Numerical Mathematics, Russia	4° × 5°L21	1979–2003	1
MIROC3.2 (medres)	CCSR/NIES/FRCGC, Japan	T42L20	1979–2002	1
MPI-ECHAM5	Max Planck Institute for Meteorology, Germany	T63L32	1978–1999	3
MRI-CGCM2.3.2a	Meteorological Research Institute, Japan	T42L30	1979–2002	1

Though the rotation amplitude is as large as 360°, the rotation direction is completely reverse. It rotates counter-clockwise from its winter state (Jan 1–Jun 1) to its summer state (Jun 10–Sep 8), and continuously rotates counter-clockwise to its initial state. This suggests that the rotation amplitude of the wind vector in an annual cycle is not always between 0° and 180° as the absolute angle defined. Meanwhile, the absolute angle is not able to detect and describe the rotation direction of the wind vector. Therefore, here, we introduce the concept of directed angle, which is a signed measure of the angle. It has the ability to distinguish different rotation directions and amplitudes to describe the whole process of wind vector rotation. In this study, we define the counter-clockwise (clockwise) rotation as the positive (negative) value of the angle. Considering the gradual change of climatological daily wind vectors, we adopt a day-to-day recursion method to calculate the daily directed angle α as follows:

$$\alpha_1 = \alpha(\mathbf{V}_1, \mathbf{V}_R) = \delta\beta_1, \tag{2}$$

$$\alpha_i = \alpha(\mathbf{V}_i, \mathbf{V}_R) = \alpha_{i-1} + \delta\beta(\mathbf{V}_i, \mathbf{V}_{i-1}), \quad (i = 2, ..., 365) \tag{3}$$

where δ is the signed function to determine the rotation direction and $\mathbf{V}_R$ is the reference wind vector (we choose the January climatological wind vector). If $\mathbf{V}_i(\mathbf{V}_1)$ is in the clockwise (counter-clockwise) direction of $\mathbf{V}_{i-1}(\mathbf{V}_R)$, then $\delta = -1(1)$. β is the absolute angle between the specific day and the day before. From the calculated formulation, it can be seen that the concept of directed angle contains the rotation direction of the wind vector, which is much more visual and objective than the absolute angle to investigate variations in wind direction.

3 Rotation styles of global wind vectors with seasonal evolution

3.1 Examples of season evolution of wind direction described by the directed angle

Based on the definition of directed angle, the variations in global wind vectors have been examined. Here, several examples of the directed angle and absolute angle of wind vectors are shown in Fig. 1. Since the wind direction is an important factor to characterize a monsoon, we focus first on the seasonal evolution of the monsoon. Then, four different rotation phenomena are detected over monsoon domains. This implies that the seasonal reversals of wind vectors are characterized by different rotation directions and amplitudes in different regions. The first species is similar to the point at (7.5°N, 112.5°E; see Fig. 2a). According to the definition of directed angle, the curve indicates that the wind vector rotates first clockwise from January to June. After stabilizing at nearly –180° for a few days, it rotates counter-clockwise to its initial state. So, this rotation style is defined as (1) clockwise to counter-clockwise (CTCC) rotation. However, this rotation feature cannot be obtained from the curve of absolute angle. The second species is completely the opposite to the first (see Fig. 2b). Since the daily rotation angle at (5°N, 85°E) is

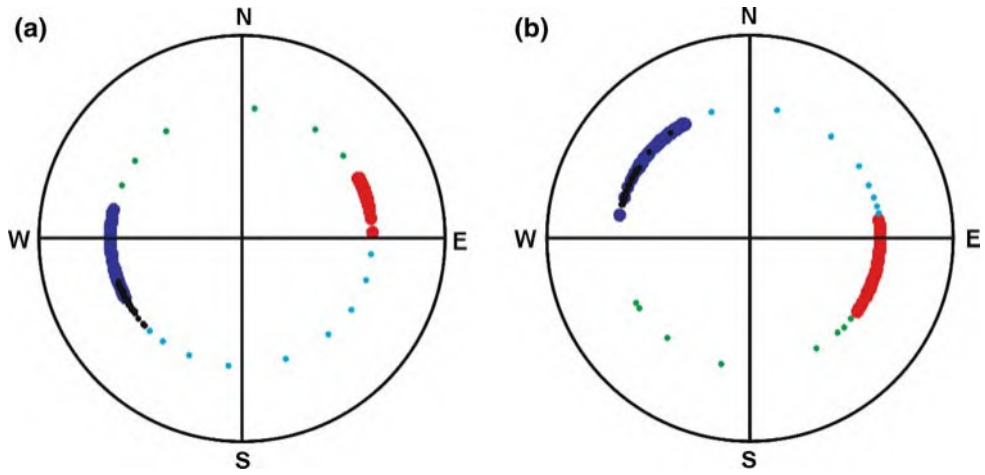

Fig. 1 Scattered representation of wind direction of normalized wind vector in the annual cycle at **a** 10°N, 55°E: *blue big dots* represent day 1–129 (Jan 1–May 9); *green small dots* represent day 130–135 (May 10–15); *red big dots* represent day 136–281 (May 16–Oct 8); *cyan small dots* represent day 282–290 (Oct 9–17); *black small dots* represent day 291–365 (Oct 18–Dec 31); indicating full clockwise rotation with seasonal evolution. **b** 15°N, 45°E: *blue big dots* represent day 1–152 (Jan 1–Jun 1); *green small dots* represent day 153–160 (Jun 2–9); *red big dots* represent day 161–251 (Jun 10–Sep 8); *cyan small dots* represent day 252–259 (Sep 9–16); *black small dots* represent day 260–365 (Sep 17–Dec 31); indicating full contour-clockwise rotation with seasonal evolution

positive and the directed angle increases gradually at first, it denotes that the wind vector rotates counter-clockwise from January to June. Subsequently, the directed angle decreases, and that implies the daily rotation angle is negative and the wind vector rotates clockwise from September to December. It is defined as (2) counter-clockwise to clockwise (CCTC) rotation. Though both curves of directed angle and absolute angle in Fig. 2b seem identical, they have different physical meanings. From the curve of directed angle, it is easy to detect the rotation direction of the wind vector. But for the absolute angle, it always increases from winter to summer and decreases from summer to winter. In the above examples, if the wind vector rotates counter-clockwise (clockwise) less than 180° at first, and then clockwise (counter-clockwise) afterward, the absolute angle and the absolute values of directed angle are consistent. The other two species of rotation styles are the same as the point at (10°N, 55°E; see Fig. 2c) and (15°N, 45°E; see Fig. 2d). As showed in Fig. 1, the wind vector rotates clockwise or counter-clockwise in the annual cycle. These two styles are defined as (3) full clockwise (FC) rotation and (4) full counter-clockwise (FCC) rotation, respectively. In these two rotation styles, though the monsoon wind vector rotates back to its initial state, it has actually rotated almost 360°. Therefore, the curves of directed angle in Fig. 2c and d are able to describe well the whole rotation feature. However, we cannot obtain any additional information about the rotation direction and rotation amplitude from the curve of absolute angle; and this is the key discrepancy between directed angle and absolute angle. Furthermore, the absolute angle and the absolute values of directed angle are not consistent under these two circumstances.

Comparing monsoon regions, variations in wind vectors are different in atypical monsoon regions. According to the curves of directed angle, the rotation styles have their own features. Though the variations of curves in atypical monsoon regions exhibit instability and much fluctuation, there are the four rotation styles mentioned above, too. Besides, two other distinct rotation styles occur in atypical monsoon regions. One is (5) stable rotation, and the other is (6) unstable rotation. The former is similar to the point at (10°S, 340°E) where the variation in wind direction is inconspicuous. In addition, the wind vector always fluctuates around the reference wind vector (Fig. 2e) with the maximal angle less than 10°. The latter is similar to the point at (62.5°N, 40°E; see Fig. 2f). The wind vector sometimes rotates clockwise, but sometimes counter-clockwise and the variation in wind direction is unpredictable, without an obvious rotation direction in the annual cycle. It is notable that directed angle is better than absolute angle in representing fluctuating amplitude.

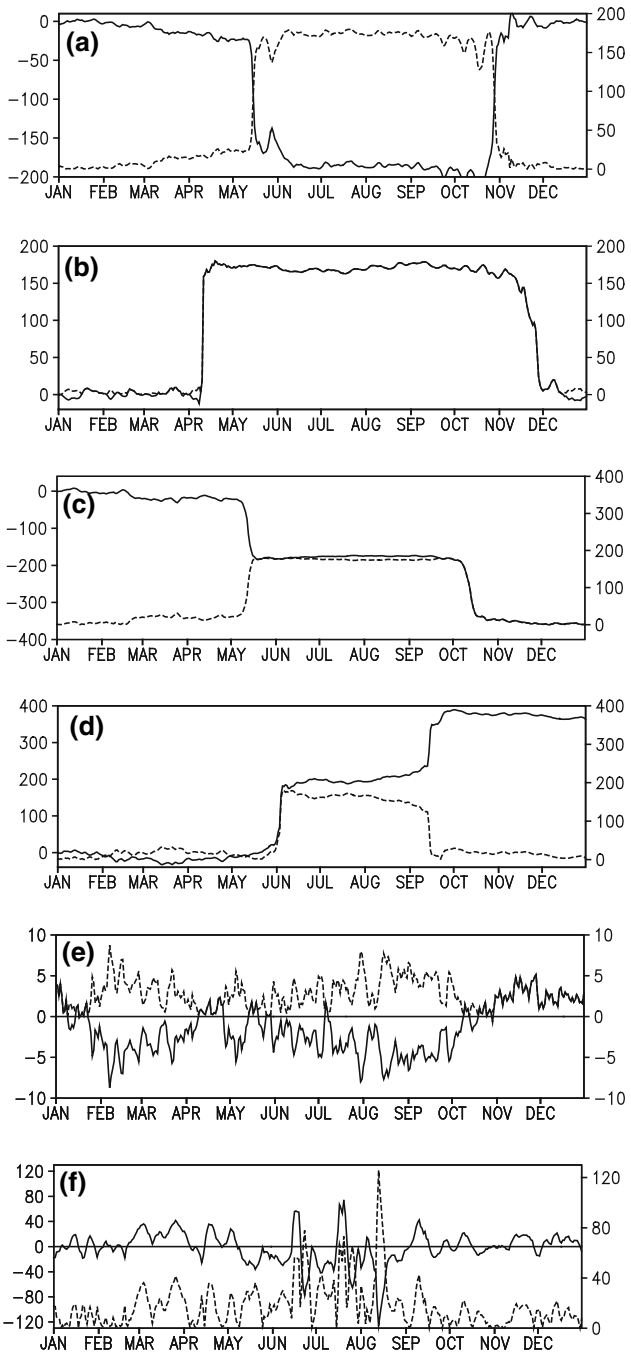

Fig. 2 Seasonal variation of directed angle (*solid line*) and absolute angle (*dashed line*) of wind vectors at **a** 7.5°N, 112.5°E; **b** 5°N, 85°E; **c** 10°N, 55°E; **d** 15°N, 45°E in monsoon regions and **e** 10°S, 340°E; **f** 62.5°N, 40°E in atypical monsoon areas. The directed angle is shown on the left axis; the absolute angle is shown on the right axis. Unit: degrees

3.2 Classification of seasonal rotation of wind vector

According to the different seasonal evolution of the directed angles in the global, six categories of wind vector rotation styles are classified as follows:

1. CTCC rotation: The leading rotation of the wind vector is clockwise from winter to summer, but counter-clockwise from summer to winter.
2. CCTC rotation: The leading rotation of the wind vector is counter-clockwise from winter to summer, but clockwise from summer to winter.
3. FC rotation: The leading rotation of the wind vector is clockwise during the whole year. In total, it rotates by around –360°.
4. FCC rotation: The leading rotation of the wind vector is counter-clockwise during the whole year. In total, it rotates by around 360°.
5. Stable style: The wind vector always fluctuates near the reference wind vector, and the amplitude of the directed angle is very small (≤±20°). This is coincident with the trade wind in the tropics.
6. Unstable style: The wind vector has neither notable rotation direction nor a stable maintainable period. The rotation direction varies quickly between clockwise and counter-clockwise and the maximal directed angle is more than ±20°.

3.3 Global distribution of rotation regimes of wind vectors

The above six categories basically capture the rotation direction of the global wind vector with seasonal evolution. In terms of this classification, Fig. 3 shows the global distribution of 850 hPa wind vector rotation regimes. The rotation styles of the wind vectors have a distinct regional distribution and interlaced zonal properties. The distribution patterns of the rotation regimes are as follows:

The rotation styles CTCC and CCTC cover most areas with an obviously interlaced zonal pattern. The CTCC is mainly located in central Eurasia, in the eastern North Pacific, and in the central North Atlantic. In addition, the eastern tropical Pacific, northern South America, the northern South Indian Ocean, as well as some high latitude areas of the Southern Hemisphere, are also covered by this style. The domain of CCTC rotation primarily lies on the eastern shores of the Eurasian continent, in the western North Pacific, in central and eastern North America, as well as in South Asia and the Arctic.

Comparatively, only are a few areas are covered by the styles FC and FCC. The style FC centers on the vicinal regions of the South Asian monsoon, such as the Indo-China Peninsula, to the south of the Philippines, and in central Africa. The style FCC is mainly distributed along the eastern shores of China, in the Bay of Bengal, and in some parts of the Artic. In addition, there are fragmentary distributions of the styles FC and FCC in other areas.

The stable style covers a continuous and large distribution. Its domain in the tropics exhibits a northwest–southeast orientation, which is consistent with the trade wind zone. Since seasonal variations in trade wind directions are much smaller, this may contribute to the formation of the stable rotation style.

In the Northern Hemisphere, the unstable style mainly converges in the west of the Eurasian Continent, along the eastern shores of the North Atlantic, in northeastern North America, central North Pacific, and western Siberia, as well as in the central Arctic Ocean. In the Southern Hemisphere, however, it is mainly located in the area from 180°E to 120°W of the westerly belt. Furthermore, the unstable style covers the boundary between the style CTCC and the style CCTC, and the distributions of the unstable style in the

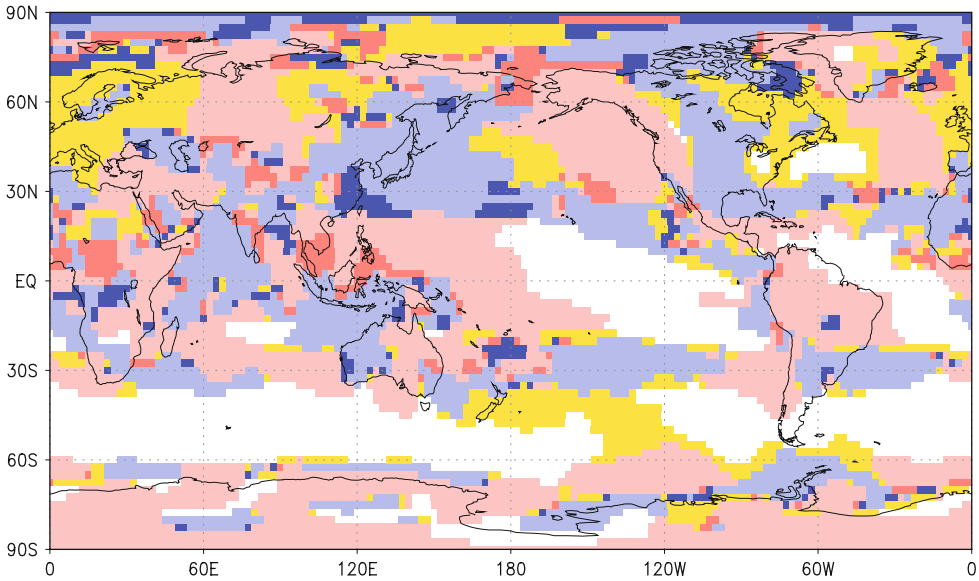

Fig. 3 Global rotation regimes of wind vectors with seasonal evolution at 850 hPa. Style I, clockwise to counter-clockwise (*CTCC*) rotation, is shown in *light red*; style II, counter-clockwise to clockwise (*CCTC*) rotation, is shown in *light blue*; style III, full clockwise (*FC*) rotation, is shown in *deep red*; style IV, full counter-clockwise (*FCC*) rotation, is shown in *deep blue*; style V, stable rotation, is shown in *white*; and style VI, unstable rotation, is shown in *yellow*

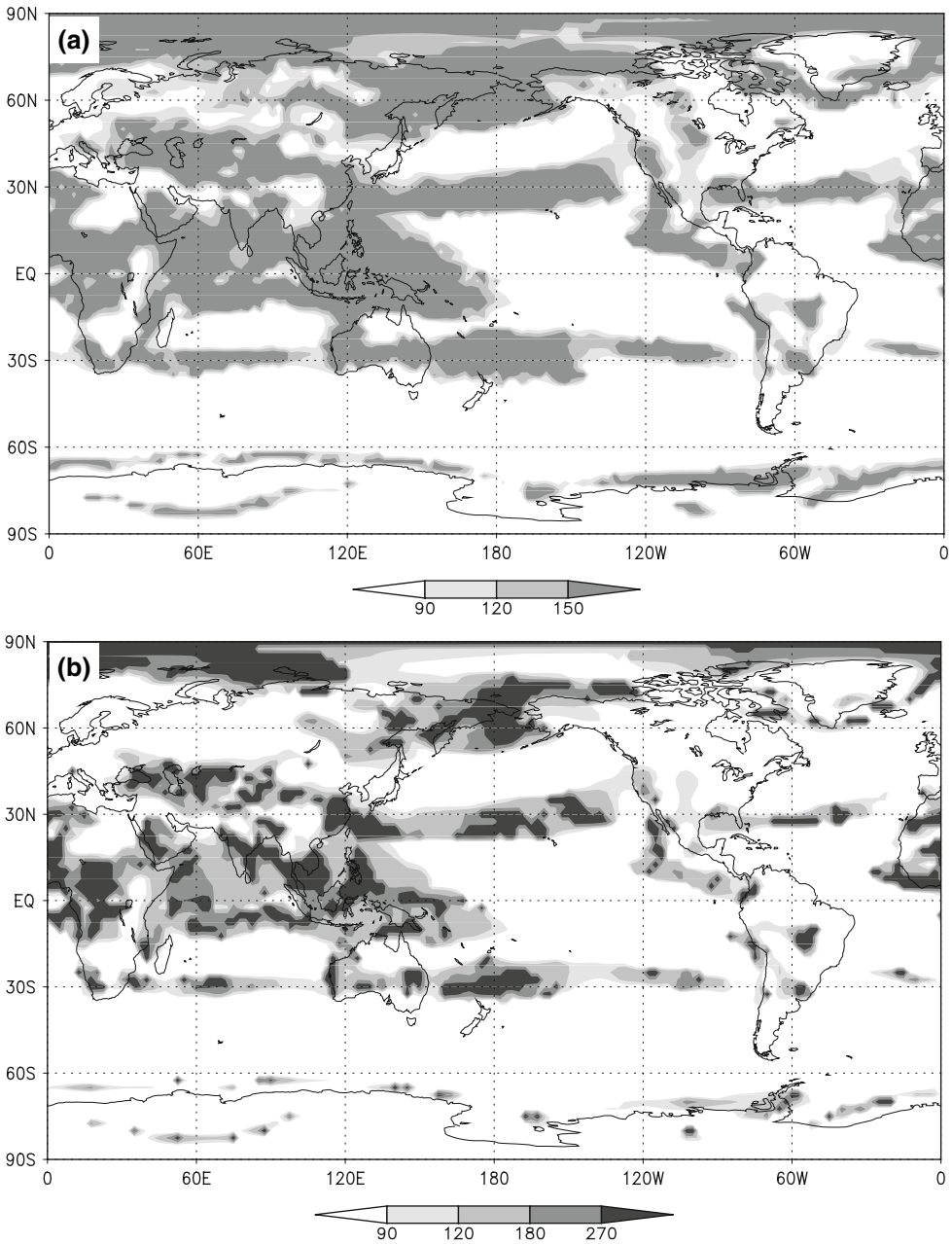

Fig. 4 Maximum amplitudes of **a** absolute angle and **b** directed angel. Unit: degrees

Atlantic and in western North America are similar to the area where storm tracks occur frequently (Blackmon 1976, 1977; Lau and Nath 1987; Lau 1988). This implies that the unstable style may be associated with transient synoptic systems on subweekly timescales, such as storm tracks which depict fluctuations in the level of synoptic-scale activities.

From the above global pattern of rotation regimes, it is clear that the pattern in the Northern Hemisphere greatly differs from that in the Southern Hemisphere, particularly in the mid latitudes. This is possibly related to the distinction between the two hemispheres in terms of land–sea distribution and the influence of topography.

Aside from the rotation direction, the rotation amplitude is another important aspect for the variation of wind vectors. As shown in Fig. 4a, the maximum absolute angle in the annual cycle is mainly divided into two intervals, 0°–90° and 150°–180°, which cover the great majority of the global. Compared to previous studies, the regions where the maximum values are more than 90° are close to the global monsoon domains defined by Khromov (1978) and Li and Zeng (2003). However, according to Fig. 2, the rotation amplitudes of wind vectors in monsoon regions are not always uniform, and the actual rotation amplitudes in some regions are not confined to between 0° and 180° in the annual cycle. Since the directed angle can reflect the

rotation amplitude of wind vectors in the annual cycle no matter how much it rotates. It can be seen from the maximum rotation amplitude of the directed angle (Fig. 4b) that there are notable differences for the rotation amplitude of wind vectors not only in monsoon domains but also in other regions. The rotation amplitude of wind vectors is more than 180° in most Asian monsoon regions, such as in Southwest China, the western Arabian Sea, the Indo-China Peninsula, and in the vicinity of the Philippines. Moreover, some of the wind vectors even have large rotation amplitudes of more than 270°. Therefore, wind vectors have regional differences in rotation amplitude which cannot be described and detected by the absolute angle.

4 Rotation regimes and annual evolution of wind direction over monsoon regions

4.1 Relationships between rotation regimes and monsoon subsystems

Although there is a regional difference in the global rotation regime, it is not divided by the boundary between monsoon regions and non-monsoon regions, and the Asian monsoon regions are mainly dominated by four rotation styles. Furthermore, we notice an interesting phenomenon in that distributions of different rotation styles in monsoon regions are related to the monsoon subsystems.

Focusing on the tropical Asian monsoon domain in Fig. 3, this indicates that the monsoon wind vector rotates counter-clockwise in the areas to the east of 80°E, but clockwise to the west of 80°E. Relatively, Li and Zeng (2002) divided the South Asian monsoon domain into two independent subsystems based on different rainfall characters, and the boundary is also near to 80°E. Furthermore, it is well known that the Asian summer monsoon is separated into two independent subsystems of the East Asian monsoon and the South Asian monsoon by a boundary near to 100°E (Tao and Chen 1987; Chen et al. 1991, 2004; Qian et al. 2004). In addition, the East Asian monsoon subsystem can be divided into the South China Sea-western Pacific tropical monsoon and the Chinese mainland-Japan subtropical monsoon, with the boundary between them situated near to 20°N (Zhu and He 1985; Zhu et al. 1986). Correspondingly, the rotation styles of monsoon wind vectors in these subsystems are quite different to each other. Therefore, the rotation regimes in the Asian monsoon domain may relate to characters of different monsoon subsystems. So, the formation processes of subsystems and the corresponding factors influencing them would be important in affecting the rotation styles of wind vectors. For instance, the properties of the East Asian monsoon are different from those of the South Asian monsoon, which is not only related to cross-equatorial flows but is also influenced by the subtropical high (Tao and Chen 1987; Wang and Ding 2006). Thus, northeasterlies rotate clockwise into southeasterlies, with the subtropical high retreating eastwards from winter to summer. Sequentially, this then rotates clockwise into southwesterlies with the advance of cross-equatorial flows from the Southern Hemisphere. This may be the reason why the rotation regime of the style CTCC covers the tropical western Pacific, the South China Sea, and the Bay of Bengal. The low level of the Arabian Peninsula was controlled by an anticyclone in winter; it shows northerlies in the Arabian Sea (Chen et al. 1991). Whereas, according to the contrast in surface friction between East Africa and the sea, it is essential for the jet's existence (Hoskins and Rodwell 1995), which may contribute to the intense cross-equatorial flows with southwesterlies in summer. As a result, with the weakening and disappearance of the anticyclone from winter to summer, the wind vector rotates counter-clockwise in the Arabian Sea, where covered by the style CCTC. So, the rotation style of wind vectors is another important element to represent the differences between monsoon subsystems.

4.2 Annual evolution of wind direction over monsoon regions

For further detecting the rotation regimes and corresponding wind direction variation in monsoon domains, we focus on the boreal major monsoon systems, which can represent well the dominant monsoon feature. According to the different rotation styles of wind vectors (Fig. 3), the monsoon-domain-averaged directed angle is defined as the area-weighted average of five rectangular boxes: South Asia (0°–20°N, 50°–80°E); East Asia (20°–40°N, 115°–140°E); the South China Sea (0°–20°N, 110°–120°E); the South Indo-China Peninsula (2.5°–15°N, 97.5°–110°E); and West Africa (5°–15°N, 20°W–40°E).

The directed angles of five major boreal monsoon domains are shown in Fig. 5. The curve in South Asia (Fig. 5a) indicates that the wind vector rotates counter-clockwise from winter to summer and then clockwise from summer to winter. It clearly belongs to the style CCTC, and the maximum rotation amplitude is almost 180°. Moreover, it is interesting that two notable turnings in the directed angle curve occur near the periods of monsoon onset and withdrawal. This implies that the wind direction changes obviously with seasonal evolution in this area. In East Asia (Fig. 5b), the variability of the directed angle in the annual cycle is quite different from that in South Asia. Firstly, the rotation style in East Asia is FCC, rotating almost 360° in the annual cycle. Secondly, there is no obvious turning in the directed angle curve at the time of monsoon commencement. Although the maximum rotation amplitude of

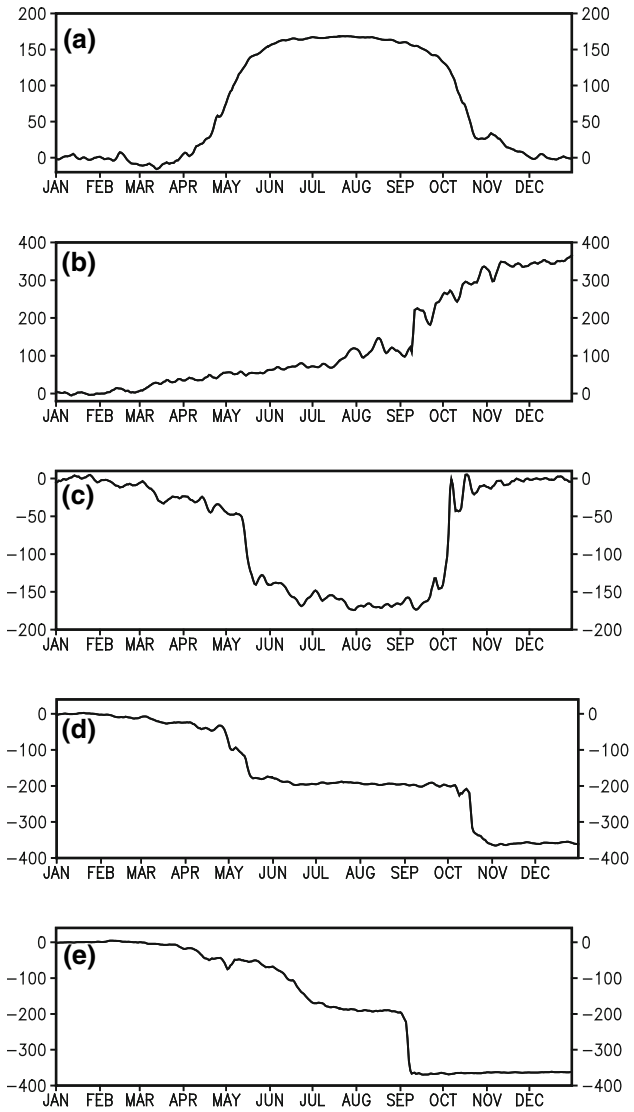

Fig. 5 Annual variation in area-averaged directed angles of wind vectors in five monsoon sectors: **a** South Asia (0°–20°N, 50°–80°E); **b** East Asia (20°–40°N, 115°–140°E); **c** South China Sea (0°–20°N, 110°–120°E); **d** South Indo-China Peninsula (2.5°–15°N, 97.5°–110°E); **e** West Africa (5°–15°N, 20°W–40°E). Unit: degrees

the South China Sea (Fig. 5c) is consistent to that of South Asia, the rotation direction is completely inverted. Similarly, the wind vector also shows notable seasonal reversal in the South China Sea. Both of the rotation styles of the wind vectors in the South Indo-China Peninsula (Fig. 5d) and in West Africa (Fig. 5e) belong to the style FC, and the maximum rotation amplitudes are close to 360°; but the first turning is not notable in the curve of West Africa compared to that of the former. Moreover, the time when the first turning occurs in the South Indo-China Peninsula is much earlier than that of West Africa. This may be associated with the fact that there are several rotation styles co-emerging in West Africa (see Fig. 3), which possibly influences the area-averaged wind direction.

Though it is hard to understand why the wind vectors in some of the monsoon domains have different rotation directions and amplitudes, the primary spatio-temporal properties of wind vectors at the daily timescale are characterized by their own features. Fortunately, the directed angle is able to describe and reveal the inimitable features and indicate the behavior of the seasonal reversal for monsoon wind direction, which may provide a new clue for monsoon research. Furthermore, it can be used as a new metric to evaluate monsoon simulation since the variation of wind vectors is vital for monsoons. To some degree, it is indeed important for climate models to reproduce the rotation processes of wind vectors on a daily scale.

5 Performance of AGCMs in simulating the rotation regimes and evolution of monsoon wind vectors

5.1 Simulating global rotation regimes of wind vectors

This section applies the new concept of directed angle in evaluating the model outputs of eight AGCMs of AMIP in the IPCC AR4 and examines to what extent the models can reproduce the rotation styles of wind vectors. Figure 6 shows the performance of each model in simulating the global distribution of 850 hPa wind vector rotation styles. And Table 2 summarizes the performance of each model in simulating different rotation styles of wind vector identified from observations. Here, the results of BCC-CM1, IAP-FGOALS-1.0 g and MPI-ECHAM5 are respective ensemble means. Meanwhile, further analysis shows there are no obvious distinctions between ensemble means and single experiments (figure not shown). In particular, the three single experiments of IAP-FGOALS-1.0 g and MPI-ECHAM5 are basically consistent with their ensemble means.

All of the models basically simulate the global distribution pattern reasonably well, apart from BCC-CM1 (Fig. 6a). The rotation styles simulated by BCC-CM1 differ from the observation in most regions, particularly the Asian monsoon region, for both the ensemble mean and in the four single experiments. In addition, it could not capture the distribution of the stable style in the trade wind region and westerly belt of the Southern Hemisphere. The rotation pattern of FCC also failed to reproduce in the North Pacific. Several models, such as CNRM-CM3 (Fig. 6b), GISS-MODEL_E_R (Fig. 6c), IAP-FGOALS-1.0 g (Fig. 6d), INMCM3.0 (Fig. 6e), and MPI-ECHAM5 (Fig. 6g) simulate the styles CTCC and CCTC well in the Northern Hemisphere; the other group of models, including MIROC3.2 (medres) (Fig. 6f) and MRI-CGCM2.3.2a (Fig. 6h) fail to reproduce well the rotation styles in the Eastern Asia. For the styles FC and FCC, just a few models

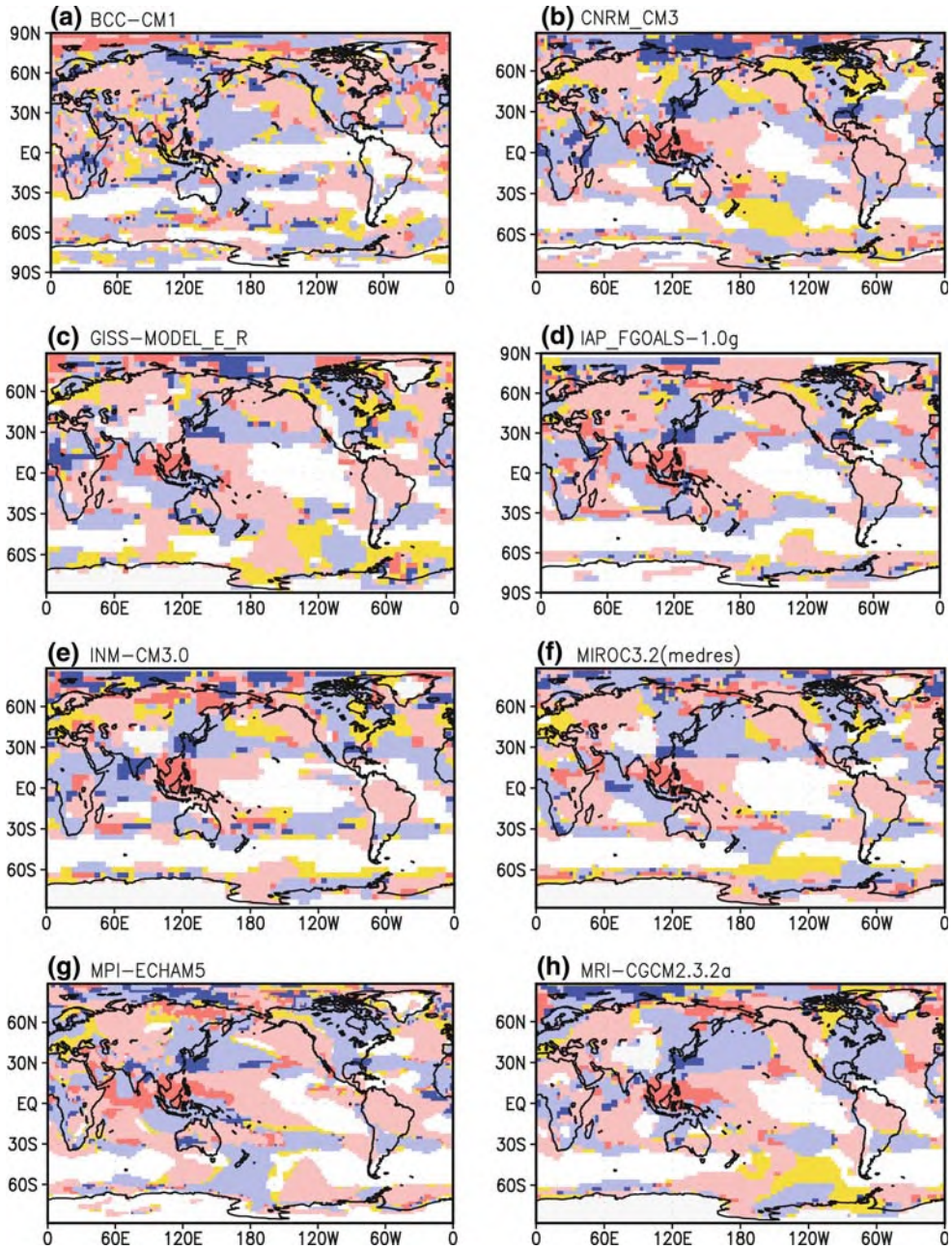

Fig. 6 As in Fig. 3 but for the model simulations and gray denotes a missing value. **a** BCC-CM1; **b** CNRM-CM3; **c** GISS-MODEL_E_R; **d** IAP-FGOALS-1.0 g; **e** INM-CM3.0; **f** MIROC3.2 (medres); **g** MPI-ECHAM5; and **h** MRI-CGCM2.3.2a

are coincident with the observations, and only in certain areas. For instance, nearly all simulations show some unrealistical discrepancies in capturing the FC pattern in the South China Sea. And over the Bay of Bengal, the simulations of CNRM-CM3, GISS-MODEL_E_R, MIROC3.2 (medres) and MPI-ECHAM5 generate a false rotation style too. Furthermore, most models are not good at simulating the styles FC and FCC over the Arctic and the Asian monsoon domains. For the stable style, in the trade wind regions, it is better reproduced in the majority of models, except BCC-CM1. In detail, the distributions of the stable style of seasonal evolution of wind vectors in the simulations of INMCM3.0 and MRI-CGCM2.3.2a are wider over the tropics Pacific than those of the observations, but those of the MPI-ECHAM5 are narrow over the Atlantic. Over the austral westerly belt, the simulations of stable style in IAP-FGOALS-1.0 g are similar to the observations, except in the area close to 180°E–90°W. However, the ensemble means of MPI-ECHAM5 and IAP-FGOALS-1.0 g are much better than the single experiments in the austral westerly belt (figure not shown). It is noted that most models are not able to simulate the unstable style pattern over the western Eurasian continent except MIROC3.2 (medres). However, CNRM-CM3,

Table 2 Summary on the performance of AMIP models in Table 1 in simulating different rotation styles of wind vector

Model	Rotation Type					
	CTCC	CCTC	FC	FCC	Stable style	Unstable style
BCC-CM1	+ ENP (EA) – most areas	+ (WNP) – most areas	+ ICP – most areas	+ CA – most areas	+ (ATWA) – most areas	+ CNP – most areas
CNRM-CM3	+ most areas – AWB, NEA SCS, BOB	+ most areas – (CSP)	+ ICP, SP – SCS, BOB CA	+ (ESC) – CNP, BOB	+ PTWA (AWB) – ATWA	+ CNP (AWB), NEA – WEC
GISS-MODEL_E_R	+ most areas – AWB, SCS BOB	+ most areas – AWB	+ ICP (SP) – SCS, BOB CA, AS	+ WNP – ESC, CNP BOB	+ PTWA – AWB, ATWA	+ (AWB) – WNA, EC
IAP-FGOALS-1.0g	+ most areas – WNA, SCS	+ most areas – CA	+ ICP, SP – SCS	+ ESC – BOB	+ PTWA, AWB – ATWA	+ (CEC) – AWB, WEC, WNA
INM-CM3.0	+ most areas – WSP, SCS	+ most areas – CA	+ ICP, SP – SCS	+ ESC – ISC, WNP	+ AWB, ATWA – PTWA	+ CNP – AWB, (WEC)
MIROC3.2 (medres)	+ most areas – SCS	+ most areas – AWB, EA	+ ICP, SP – SCS	+ ESC – WNP, BOB	+ (PTWA) – (AWB), (ATWA)	+ CNP – WNA, (AWB)
MPI-ECHAM5	+ most areas – AWB, SCS BOB	+ most areas – AWB, AS	+ ICP, SP – BOB, AS, CA	+ WNP, CNP – ESC	+ PTWA – AWB, ATWA	+ CEC – AWB, WNA, (WEC)
MRI-CGCM2.3.2a	+ most areas – AWB, SCS	+ most areas – EA, NA	+ ICP (SP) – SCS, CA	+ WNP – ESC	+ PTWA, ATWA – AWB	+ (AWB) – WEC, WNA,

The symbols and abbreviations are as follows: + Simulate reasonablely well; – Simulate unreasonablely well;

(*X*) Part of a certain area X; *AS* Arabian Sea; *AWB* Austral westerly belt; *ATWA* Atlantic trade wind areas; *BOB* Bay of Bengal; *CA* Central Africa; *CEC* Central Eurasia continent; *CNP* Central North Pacific; *CSP* Central South Pacific; *EA* Eastern Asia; *ENP* Eastern North Pacific; *ESC* Eastern shore of China; *ICP* Indo-China Peninsula; *ISC* Indian subcontinent; *NEA* Northeastern America; *NA* North Atlantic; *PTWA* Pacific trade wind areas; *SCS* South China Sea; *SP* Southern Philippines; *WNA* Western North America; *WEC* Western Eurasian continent; *WNP* Western North Pacific; *WSP* Western South Pacific

Table 3 Correlation coefficients between the simulated and the observed directed angle over monsoon regions

Model	Regions				
	South Asia	East Asia	South China Sea	South Indo-China Peninsula	West Africa
BCC-CM1	**–0.47**	–0.19	–0.11	**0.83***	**0.55**
CNRM-CM3	**0.94***	**0.93***	0.14	**0.99***	0.17
GISS-MODEL_E_R	**0.93***	**0.95***	**0.87***	**0.96***	–0.07
IAP-FGOALS–1.0 g	**0.95***	**0.97***	0.92*	**0.97***	0.01
INM-CM3.0	**0.99***	**0.96***	**0.83***	**0.99***	–0.05
MIROC3.2 (medres)	**0.97***	**0.98***	0.03	**0.99***	**0.93***
MPI-ECHAM5	**0.97***	**0.96***	0.14	**0.97***	**0.94***
MRI-CGCM2.3.2a	**0.62***	**0.92***	–0.06	**0.89***	**0.38**
Ensemble mean (without BCC-CM1)	**0.95***	**0.94***	0.10	**0.99***	0.17

Bold numbers are correlations significant at the 99% confidence level; and * represents the same rotation style as the observed

GISS-MODEL_E_R, and MRI-CGCM2.3.2a reproduce the unstable style rotation over the austral westerly belt reasonably well.

Therefore, though seven of the eight models generally capture the global distribution pattern of wind vector rotation, there are also shortcomings in some regions. In

particular, simulation in the Asian monsoon regions still needs to be improved, which is important in studying monsoons and global climate. In addition, the performance in simulating the stable style in the trade wind regions is reasonably good in a few models, while the simulation of the unstable style is not particularly realistic in the majority of models. Little improvement is shown in the ensemble mean compared to single experiments, which is similar to the simulation of monsoon precipitation in ECMWF (Wang 1997). Only simulations in a few regions, such as the austral westerly belt, are better than the single experiments.

5.2 Performance in simulating seasonal variation of wind vector rotation over monsoon sectors

Because of the various spatial resolutions in the AGCMs' simulations and observations, direct comparisons must be based on a common grid mesh that is most representative of the suite of data used and the regional climate characteristics to be studied (Liang and Wang 1998). In order to further discuss the regional difference in monsoon regions and the variation of monsoon wind vector rotation, we will evaluate the simulation in five major monsoon domains in this section. According to the above simulation results, the simulation of BCC-CM1 will not be further discussed because of its great difference from the observation. Also, the all-model composite of climatological mean wind is made by averaging the seven model results without BCC-CM1.

As a comparison, Fig. 7a indicates the simulations and observations of directed angles in South Asia. All models reproduce the CCTC well in the annual cycle. The exception is MRI-CGCM2.3.2a, of which the variation of directed angle is not very consistent with the observed. That is quite different to the couple model of MRI-CGCM2.3.2 which appears to be most realistic to simulate the annual cycle of precipitation over the south Asian monsoon region in the experiments of climate of the twentieth century (20c3m) of IPCC AR4 (Annamalai et al. 2007). In East Asia (Fig. 7b), where the FCC occurs, and in the South Indo-China Peninsula (Fig. 7d), where the style FC occurs, all models simulate the corresponding rotation style correctly. For the CTCC in the South China Sea, only three models (GISS-MODEL_E_R, IAP-FGOALS-1.0 g and INMCM3.0) capture its feature (Fig. 7c), while the other models and model ensembles fail to simulate the FC. Figure 7e shows that there is great discrepancy between model simulations in West Africa. Only MIROC3.2 (medres) and MPI-ECHAM5 accurately capture the style FC.

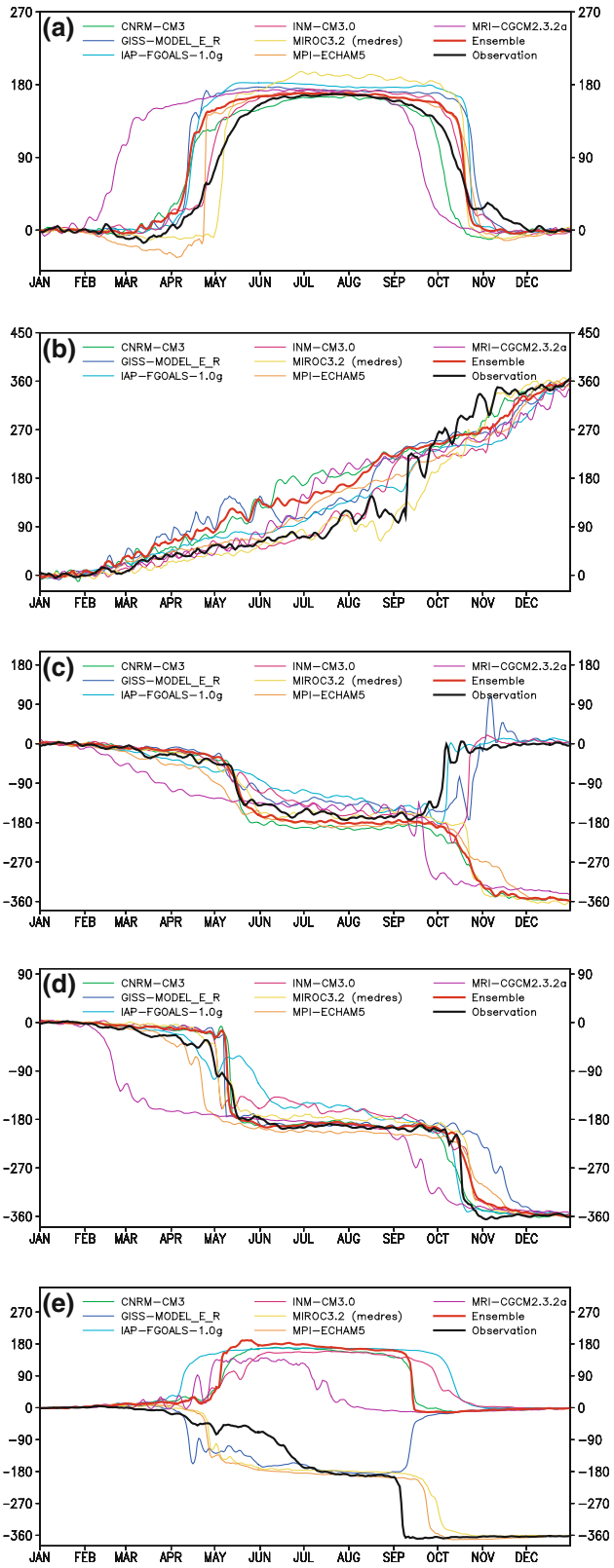

Fig. 7 As in Fig. 5 but for the comparison between simulations and observations with seasons

The rotation style simulation of the all-model ensemble differs substantially from the observed in the South China Sea and West Africa, which implies that it is still difficult for some models to reproduce the variability of wind vectors in the monsoon subsystems.

Correlation coefficients between the observed and the simulated directed angle for different models and model ensembles from January to December are listed in Table 3. Generally, in South Asia, East Asia and the South Indo-China Peninsula, there are good correlations between observations and most simulations, except BCC-CM1. In particular, the correlation coefficients of the simulated directed angle between INMCM3.0 and observations are greater than 0.96. For the IAP-FGOALS-1.0 g, the correlation between simulation and observation is highest in the South China Sea. However, the MPI-ECHAM5 simulates best in West Africa. The low correlations in both the South China Sea and West Africa between the model ensemble and the observations suggest that it is really hard for some models to capture the variability of monsoon wind vectors in these monsoon subsystems. Comparatively, GISS-MODEL_E_R, IAP-FGOALS-1.0 g and INMCM3.0 have much higher correlations with the observations in four monsoon regions. This may imply that these three perform better in reproducing the evolution of monsoon wind vectors in the annual cycle.

To further discuss and evaluate the simulated performance in different periods and their subseasonal variation, the differences in monsoon directed angle between observations and models (observed minus simulation) have been investigated. Figure 8 exhibits the differences between simulations and the observed, which denotes the errors with seasonal evolution in the above five monsoon domains. In South Asia (Fig. 8a), although all models capture the corresponding rotation style well, notable differences can be found in certain periods of time. The simulated directed angle is highly consistent with that of the observations in wintertime and summertime, but the largest errors appear in the transitional season near to the time of monsoon onset and withdrawal. Similar results occur in the South Indo-China Peninsula (Fig. 8d) as well. In addition, the models, which simulate the same rotation style as observed in both the South China Sea (Fig. 8c) and West Africa (Fig. 8e), also have the largest biases in the transitional season. The differences are much greater in the period of monsoon withdrawal in East Asia and persist for a long time. For the models which fail to simulate the rotation style in the South China Sea and in West Africa, the shortcomings in the transitional season may contribute to inaccurate rotation styles. Therefore, decreasing the errors in the transitional season could be vital in improving simulations of wind

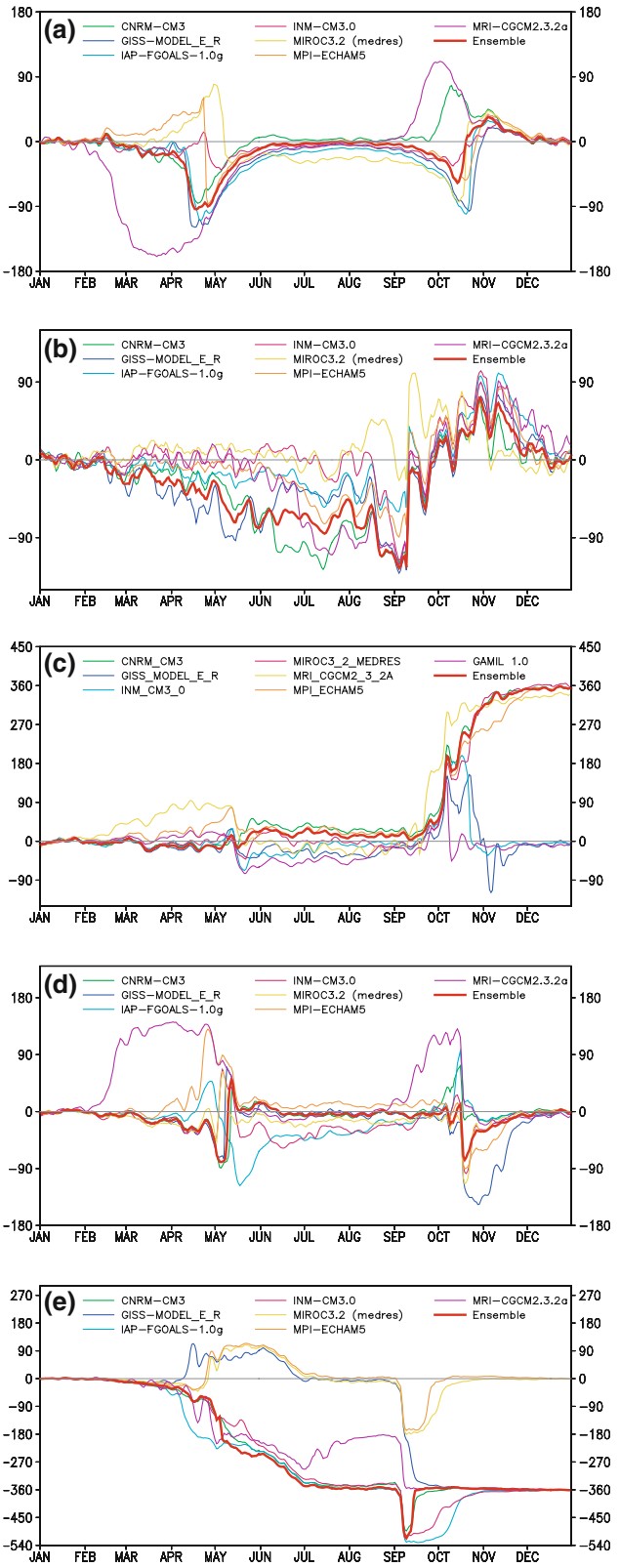

Fig. 8 As in Fig. 7 but for the biases between simulations and observation (observation minus simulation) with seasons

vector rotation regimes. Besides, it can also improve the transition time of monsoon wind direction.

6 Summary and discussion

6.1 Summary

According to the important influence of the variability of wind on global circulation and monsoon systems, we have analyzed the evolution of wind vectors in the annual cycle by introducing a new concept of directed angle. It aims at investigating and detecting the essential features of monsoon wind vectors in spatio-temporal evolution, and uses it as a metric to evaluate model simulation of monsoons on a daily scale. The results have shown that directed angle is better than absolute angle for describing the variability of wind vectors, and the evolution of global wind vectors in the seasonal cycle can be classified into six categories as follows: (1) clockwise to counter-clockwise (CTCC) rotation; (2) counter-clockwise to clockwise (CCTC) rotation; (3) full clockwise (FC) rotation; (4) full counter-clockwise (FCC) rotation; (5) stable style and (6) unstable style. In particular, the wind vector in monsoon regions rotates in accordance with the first four categories. This confirms that the rotation direction and rotation amplitude of wind vectors have regional differences. Particularly for the maximum rotation amplitude of the wind vector, only directed angle can actually indicate the rotation degree. From the rotation regimes in the Asian monsoon domains, this shows that the wind vector belonging to monsoon subsystems have their own rotation styles. The wind vectors of the five major monsoon domains in the Northern Hemisphere indicate completely different rotation styles.

In this study, we attempted to validate the simulated variability of monsoon wind vectors. Since the directed angle is able to describe the inimitable features of monsoons and indicate how monsoons achieve their seasonal reversal on a daily scale, it has been applied to evaluate the model output of eight AGCMs of AMIP in the IPCC AR4 as a new metric. The results have shown that although most models can generally simulate the global rotation regimes of wind vectors, little improvement is shown in the ensemble mean compared to single experiments. Moreover, none of the models were able to capture well the boundary among different monsoon subsystems. A few models had difficulty in simulating the rotation styles in the South China Sea and West Africa. A group of models, including GISS-MODEL_E_R, IAP-FGOALS-1.0 g, INM-CM3.0, MIROC3.2 (medres) and MPI-ECHAM5, reproduced the rotation styles reasonably well over most monsoon regions. In addition, for the wind vectors in monsoon domains, the most notable differences between simulations and the observations appeared in the transitional season, which is the time closed to monsoon onset and withdrawal. This is similar for the models which were able to simulate the same rotation style as the observed.

6.2 Discussion and future scope

Although the reasons why the wind vector rotates with different styles are still uncertain, it may show an intrinsic feature of atmospheric circulation. Some studies indicate that the variabilities of wind and monsoon circulation are closely related to many factors, such as the heat source and orographic (Webster 1972; Gill 1980; Hoskins and Rodwell 1995). Meanwhile, the relationships between rotation regimes of wind vectors and the evolution of atmospheric circulation are also interesting subjects for further investigation. Fortunately, the directed angle is able to describe the evolution of wind vectors on a daily scale, which provides a new clue for spatial and temporal information about wind vector variation. It is an important aspect for monsoon research and model evaluation, and it can also be widely used to validate other climate or synoptic phenomena which are closely associated with the variation of wind vectors, such as sea breezes. Therefore, the new concept can be used as an objective technique of phenomenological-based verification methodology to verify the variation of monsoon wind direction and can be applied to evaluate the performance of models in reproducing the variation of wind vectors on any spatial or temporal scale.

Through comparison between eight AGCMs of AMIP and observations, it has been indicated that the largest simulated errors in the transitional season may imply that the onset and withdrawal of the monsoon is the most difficult for models to reproduce. However, these two periods are most important in monsoon research because they may lead to the commencement and end of the rainy season, and accordingly affect the development of agriculture and the economy. In addition, most GCMs failed to reproduce the heavy precipitation center near India and the Bay of Bengal (Lau et al. 1996; Kang et al. 2002b), where the rotation styles of wind vectors with seasonal evolution are just dissimilar to corresponding observations. Similarly, the most of OGCMs have difficulty capturing the regional details in precipitation over India too, in particular, the high rainfall alone the west coast. And just six of the 18 models have a reasonable realistic representation of monsoon precipitation climatology (Annamalai et al. 2007). Liang et al. (2001) have confirmed that wind biases are significantly correlated with those of precipitation. Then, whether there are similar systematic errors in capturing the precipitation if there are errors of in simulating the rotation regimes? Are there any relationships and interactions

between them? These problems need further research in the future.

Acknowledgments The authors are grateful to the editor and the anonymous reviewers for their helpful comments and suggestions that greatly improved the manuscript. The authors thank Prof. Hong Liao, Dr. Min Wen and Dr. Ruifen Zhan for their help. The authors also acknowledge the international modeling groups for providing their data for analysis, the Program for Climate Model Diagnosis and Intercomparison (PCMDI) for collecting and archiving the model data, the JSC/CLIVAR Working Group on Coupled Modelling (WGCM) and their Coupled Model Intercomparison Project (CMIP) and Climate Simulation Panel for organizing the model data analysis activity, and the IPCC WG1 TSU for technical support. The IPCC Data Archive at Lawrence Livermore National Laboratory is supported by the Office of Science, U.S. Department of Energy. This work was jointly supported by the Chinese Academy of the International Partnership Creative Group entitled "Climate System Model Development and Application Studies", 973 Program (2006CB403600), and the National Natural Science Foundation of China (20221503).

References

Annamalai H, Slingo JM, Sperber KR, Hodges K (1999) The mean evolution and variability of the Asian summer monsoon: Comparison of ECMWF and NCEP-NCAR reanalysis. Mon Weather Rev 127:1157–1186

Annamalai H, Hamilton K, Sperber KR (2007) The South Asian summer monsoon and its relationship with ENSO in the IPCC AR4 Simulations. J Clim 20:1071–1092

Blackmon ML (1976) A climatological spectral study of the 500 mb geopotential height of the Northern Hemisphere wintertime circulation. J Atmos Sci 33:1607–1623

Blackmon ML, Wallace JM, Lau NC, Mullen SL (1977) An observation study of the Northern Hemisphere wintertime circulation. J Atmos Sci 34:1040–1053

Chen LX, Gao H, He JH, Tao SY, Jin ZH (2004) Zonal propagation of kinetic energy and convection in the South China Sea and Indian monsoon regions in boreal summer. Science in China (D) 34:171–179

Chen LX, Zhu QG, Luo HB, He JH (1991) Eastern Asia monsoon. China Meteorogical Press

Ding YH (1992) Summer monsoon rainfalls in China. J Meteorol Soc Jpn 70:373–396

Fennessy MJ, Kinter III JL, Kirtman B, Marx L, Nigam S, Schneider E, Shukla J, Straus D, Vernekar A, Xue Y, Zhou J (1994) The simulated Indian monsoon: AGCM sensitivity study. J Clim 7:33–43

Gadgil S, Sajani S (1998) Monsoon precipitation in the AMIP runs. Clim Dyn 14:659–689

Gill AE (1980) Some simple solutions for heat-induced tropical circulation. Quart J Roy Meteorol Soc 106:447–462

Goswami BN (1998) Interannual variations of Indian summer monsoon in a GCM: external conditions versus internal feedbacks. J Clima 11:501–522

Holton JR (2003) Encyclopedia of atmospheric sciences. Elsevier, Spain, pp 1365–1400

Hoskins B, Rodwell M (1995) A model of the Asian summer monsoon. Part I: The global scale. J Atmos Sci 52:1329–1340

Kalnay E, Kanamitsu M, Kistler R, Collins W, Deaven D, Gandin L, Iredell M, Saha S, White G, Woollen J, Zhu Y, Leetmaa A, Reynolds B, Chelliah M, Ebisuzaki W, Higgins W, Janowiak J, Mo KC, Ropelewski C, Wang J, Jenne R, Joseph D (1996) The NCEP/NCAR 40-Year Reanalysis Project. Bull Am Meteorol Soc 77:437–471

Kang IS (2004) Current status of AGCM monsoon simulations. In: Chang CP (ed) East Asian monsoon. World Scientific Publishing, Singapore, pp 301–331

Kang IS, Jin K, Lau KM, Shukla J, Krishnamurthy V, Schubert SD, Waliser DE, Stern WF, Satyan V, Kitoh A, Meehl GA, Kanamitsu M, Galin VY. Sumi A, Wu G, Liu Y, Kim JK (2002a) Intercomparison of GCM-simulated anomalies associated with the 1997/98 El Nin˜o. J Clim 15:2791–2805

Kang IS, Jin K, Wang B, Lau KM, Shukla J, Krishnamurthy V, Schubert SD, Wailser DE, Stern WF, Kitoh A, Meehl GA, Kanamitsu M, Galin VY, Satyan V, Park CK, Liu Y (2002b) Intercomparison of the climatological variations of Asian summer monsoon precipitation simulation by 10 GCMs. Clim Dyn 19:383–395

Khromov SP (1978) Great Soviet Encyclopedia (a translation of the third edition). Macmillan London, Collier Macmillan Publishers, 17:129

Krishnamurti TN (1996) Monsoons. In: Schneide SH (eds) Encyclopedia of Climate and Weather, vol 2. Oxford University Press, New York, pp 512–515

Latif M, Sterl A, Assenbaum M, Junge MM, Maier-Reimer E (1994) Climate variabilit y in a coupled GCM. Part II : The Indian monsoon. J Clim 7:1449–1462

Lau KM, Kim JH, Sud Y (1996) Intercomparison of hydrologic processes in AMIP GCMs. Bull Am Meteorol Soc 77:2209–2227

Lau NC (1988) Variability of the observed midlatitude storm tracks in relation to low-frequency changes in the circulation pattern. J Atmos Sci 45:2718–2743

Lau NC, Nath MJ (1987) Frequency dependence of the structure and temporal development of wintertime tropospheric fluctuations-comparison of a GCM simulation with observations. Mon Weather Rev 115:251–257

Lau NC, Nath MJ (2000) Impact of ENSO on the variability of the Asian-Australian monsoons as simulated in GCM experiments. J Clim 13:4287–4309

Li JP, Zeng QC (2000) Significance of the normalized seasonality of wind field and its rationality for characterizing the monsoon. Science in China (D) 30:331–336

Li JP, Zeng QC (2002) A unified monsoon index. Geophys Res Lett 29: doi: 10.1029/2001GL013874

Li JP, Zeng QC (2003) A new monsoon index and the geographical distribution of the global monsoons. Adv Atmos Sci 20:299–302

Liang XZ, Wang WC (1998) Associations between China monsoon rainfall and tropospheric jets. QJR Meteorol Soc 124:2597–2623

Liang XZ, Wang WC, Samel AN (2001) Biases in AMIP model simulations of the east China monsoon system. Clim Dyn 17:291–304

Liu YQ, Giorgi F, Washington WM (1994) Simulation of summer monsoon climate over East Asia with an NCAR regional climate model. Mon Weather Rev 122:2331–2348

Pedelaborde P (1963) The monsoon (Tr. By M.J. Clegg). Methuen, London, p 196

Qian YF, Jiang J, Zhang Y, Yao YH, Xu ZF (2004) The earliest onset area of the tropical Asian summer monsoon and its mechanisms. Acta Meteorologica Sin 62:129–139

Rajendran K, Kitoh A, Yukimoto S (2004) South and East Asian summer climate and variation in the MRI coupled model (MRI-CGCM2). J Clim 17:763–782

Ramage CS (1971) Monsoon meteorology. Academic, New York, p 296

Shukla J, Fennessy MJ (1992) Some idealised experiments to diagnose the simulated Asian summer monsoon variability, WCRP-68, WMO/TD-No. 470, Geneva, Switzerland, pp 2153–2157

Shukla JM, Fennessy MJ (1994) Simulation and predictability of monsoons. In: Proceedings of the international conference of Monsoon Variability and Prediction. Technical Report WCRP-84, WCRP, Geneva, Swizerland, pp 567–575

Sperber JM, Slingo JM, Annamalai H, (2000) Predictability and the relationship between subseasonal and interannual variability during the Asian summer monsoon. Quart J Roy Meteorol Soc 126:2545–2574

Sperber KR, Palmer TN (1996) Interannual tropical rainfall variability in general circulation model simulations associated with the Atmospheric Model Intercomparison Project. J Clim 9:2727–2750

Tao SY, Chen LX (1987) A review of recent research on East summer monsoon in China. In: Chang CP, Krishramurti TN (eds) Monsoon meteorology. Oxford University Press, Oxford, pp 60–92

Waliser DE, Jin K, Kang IS, Stern WF, Schubert SD, Wu ML, Lau KM, Lee MI, Krishnamurthy V, Kitoh A, Meehl GA, Galin VY, Satyan V, Mandke SK, Wu G, Liu Y, Park CK (2003) AGCM simulations of intraseasonal variability associated with the Asian summer monsoon. Clim Dyn 21:423–446

Wang B (2006) The Asian monsoon, 1st edn. Springer, Berlin, pp 5–377

Wang B, Ding QH (2006) Changes in global monsoon precipitation over the past 56 years. Geophys Res Lett 33:L06711, doi: 10.1029/2005GL025347

Wang HJ (1997) The advance of the atmospheric model intercomparison project (AMIP). Chines J Atmos Sci 21:633–637

Wang B, Kang IS, Lee JY (2004a) Ensemble simulations of Asian-Australian monsoon variability by 11 AGCMs. J Clim 17:803–818

Wang ZZ, Wu GX, Wu TW, Yu RC (2004b) Simulation of Asian monsoon seasonal variations with climate model R42L9/LASG. Adv Atmos Sci 21:879–889

Webster PJ (1972) Response of the tropical atmosphere to local, steady, forcing. Mon Weather Rev 100:518–540

Webster PJ (1987) The elementary monsoon, monsoons. Wiley, New York, pp 3–32

Webster PJ, Magana VO, Palmer TN, Shukla J, Tomas RA, Yanai M, Yasunari T (1998) Monsoons: processes, predictability, and the prospects for prediction. J Geophys Res 103:14,451–14,510

Zachary A, Randall D (1999) Sensitivity of the simulated Asian summer monsoon to parameterized physical processes. J Geophys Res 104:12,177–12,191

Zeng QC, Liang XZ, Zhang MH (1988) Simulation on the abrupt change of monsoon and the general circulation. Sci Atmos Sin (spec issue):22–24

Zhang Y, Sperber KR, Boyle JS, Dix M, Ferranti L, Kitoh A, Lau KM, Miyakoda K, Randall D, Takacs L, Wetherald R (1997) East Asian winter monsoon: results from eight AMIP models. Clim Dyn 13:792–820

Zhao ZC, Ding Yh, Li XD, Wang SW (1995) Evaluation of CGCM climate simulation in East Asia region. Quar J Appl Meteorol 6:9–18

Zhu QG, He JH (1985) On features of the upper circulation in the establishment of Asian monsoon in 1979 and its medium-range oscillation. J Trop Meteorol 2:9–18

Zhu QG, He JH, Wang PX (1986) A study of circulation differences between East-Asian and Indian summer monsoons with their interactions. Adv Atmos Sci 3:466–477